Original Article

Theoretical diagnosis of emphysema by aerosol bolus inhalation

Robert Sturm

Department of Materials Science and Physics, Division of Physics and Biophysics, University of Salzburg, Salzburg, Austria
Correspondence to: Dr. Robert Sturm. Brunnleitenweg 41, A-5061 Elsbethen, Austria. Email: sturm_rob@hotmail.com.

Background: The present contribution deals with the theoretical description of aerosol bolus dispersion in lungs being affected by different manifestations of emphysema. The work constructs the hypothesis that each manifestation of emphysema exhibits specific properties with regard to the dispersion of inhaled and exhaled aerosol boluses as well as the deposition of particles from the aerosol pulse.

Methods: For an appropriate simulation of single emphysematous manifestations, a previously developed model assuming (I) a random variation of alveolar diameters, (II) an exact localization of diseased structures, and (III) a realistic balance between alveolar air volume and number of air sacs was applied. Dispersion of inhaled and exhaled aerosol boluses was simulated by using the mathematical concept of effective diffusivities. Computations were conducted for an average adult lung (FRC =3,300 mL), symmetric breath-cycles with a length 8 s, and inhalation flow rates of 250 mL/s. Particles used for the model predictions had a uniform diameter of 0.84 µm and a density of 1 g/cm^3.

Results: According to the theoretical data obtained from the model highest aerosol bolus dispersion may be observed in lungs affected by panacinar and bullous emphysema, whereas centriacinar and paraseptal emphysema cause a significant reduction of the phenomenon. Also other statistical parameters exhibit partly remarkable differences among the studied manifestations. Particle deposition in lungs affected by bullous emphysema falls below that of lungs impaired by the other types of emphysema by 2%–50%.

Conclusions: From the hypothetical results presented in this study it may be concluded that aerosol bolus inhalation bears a certain potential for the diagnosis of emphysematous structures and, if applied with sufficient accuracy, also for the distinction of single manifestations of emphysema. For a successful use of the technique, however, all statistical bolus parameters and particle deposition have to be subjected to a detailed evaluation.

Keywords: Aerosol bolus; dispersion; stochastic model; lung; emphysema

Submitted Feb 06, 2017. Accepted for publication Feb 15, 2017.
doi: 10.21037/atm.2017.03.28
View this article at: http://dx.doi.org/10.21037/atm.2017.03.28

Introduction

General aspects with regard to emphysema

Emphysema ranks among those chronic lung diseases, which have remarkably attracted medical attention during the past decades (1,2). In general, this insufficiency is characterized by a slowly progressive destruction of the fragile tissues between the lung alveoli and the continuous formation of large peripheral pockets, within which a growing amount of residual air gets trapped. As a consequence of this development, the lungs permanently increase in size and breathing becomes harder. According to current medical research cigarette smoke represents the primary external cause for the abnormal distension of alveolar structures resulting from the decomposition of alveolar walls and septa (3,4). Based on the classical hypothesis, it is argued that smoke particles reaching the distal air space walls cause a considerable imbalance between the enzyme elastase and anti-elastase in favour of elastase. The neutrophil enzyme subsequently undergoes an uncontrolled synthesis, which implicates a continuous elastolysis within the alveolar walls and consequently the onset of emphysema (5,6). An alternative theory raises the elastin-based model to question and underlines the role of collagenases with regard to the destruction of alveolar tissue in emphysematous lungs (7,8).

In medical literature, four different manifestations of emphysema are described (*Figure 1*) (9). Centriacinar emphysema initially develops in the respiratory bronchiole

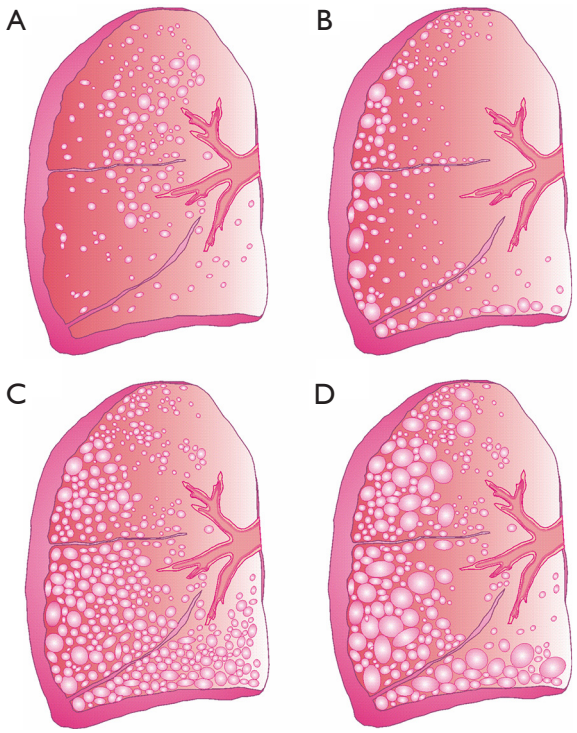

Figure 1 Main manifestations of emphysema modeled in this contribution. (A) Centriacinar emphysema; (B) paraseptal emphysema; (C) panacinar emphysema; (D) bullous emphysema.

and afterwards spreads peripherally. This type chiefly results from long-term cigarette smoking and preferentially afflicts the upper lung lobes. Paraseptal emphysema is commonly characterized by a concentration of abnormal distensions around the lung septa or pleura. Due to the circumstance that this type of emphysema primarily afflicts distal airway structures, alveolated ducts, and alveolar sacs, patients suffering from this disease are subject to an increased risk for spontaneous pneumothorax (9). Panacinar emphysema corresponds to the homogeneous destruction of the entire respiratory compartment (i.e., the structures, within which gas exchange takes place) and preferably involves the lower lung lobes. It is particularly observed in smokers suffering from a congenital deficiency of alpha-1-antitrypsin (AAT) (6). The last manifestation, bullous emphysema, may be regarded as final stage of the other three types described above and exhibits further enlargement of distal air spaces. In its most extreme form, the chronic disease develops alveoli measuring several centimeters in diameter. This, however, causes the reduction of the gas exchange surface to a minimum (10).

With regard to its pathophysiology, emphysema is frequently associated with chronic obstructive pulmonary disease (COPD), leading to remarkable modifications of the central and peripheral airway structures (9). These changes commonly result in valuable airflow limitations on the one hand and successive air trapping in the emphysematous compartment on the other. Patients developing a significant predominance of emphysema over COPD ("pink puffers") show limited pulmonary airflow due to the loss of elastic recoil in the air sacs. Contrary, patients developing a severe form of COPD but a mild form of emphysema ("blue bloaters") display bronchiolar abnormalities as main causes of airflow disturbances. The continuous destruction of peripheral lung architecture by emphysema and COPD is among other reflected by a decline of the FEV_1, which is reduced to about 30% of the value typically found in healthy probands. In addition, the FEV_1/FVC quotient normally assuming a value of 75% falls below 40% in patients with progressing lung disease (9). The quotient between residual lung volume (RV) and total lung capacity (TLC) is subject to an increase from 25% in healthy subjects to nearly 80% in patients with severe emphysema (9,11). The change of lung volumes entails the development of asymmetric breathing cycles with considerably prolonged exhalation times. The final stage of emphysema is usually marked by the development of cyanosis, elevated jugular venous pressure (JVP), peripheral edema, and right heart failure (9).

Role of aerosol bolus inhalation in pneumology

In general, an aerosol bolus represents a small volume of air (e.g., 50 mL) labelled with sub-micron test particles, which is inserted into the proband's inspiratory volume at a predefined time point (12-20). Aerosol bolus transport in the air-conducting and respiratory structures of the lungs is commonly characterized by a dispersion of the particles to adjacent air volumes in the wake of convective and diffusive processes (12,13). As a physical consequence of this phenomenon, the exhaled aerosol bolus is spread over a larger air volume than the inhaled bolus. This observation termed aerosol bolus dispersion was assessed as an easily measurable parameter showing a certain sensitiveness to specific disease-induced modifications of lung architecture (21-29).

In the past, aerosol bolus dispersion was among other investigated in smokers and compared with the bolus behaviour in age- and gender-matched nonsmokers (21). Here, it turned out that bolus dispersion in smokers surpassed that of nonsmokers by a certain degree, whilst spirometric data exhibited only slight discrepancies between the two

test groups. According to further medical studies inhaled aerosol boluses also undergo enhanced dispersion in patients suffering from cystic fibrosis (22), COPD (23-25), chronic asthma (26), and, important in the context of the present contribution, also emphysema (27-29). Vast majority of these clinical studies came to the essential conclusion that aerosol bolus dispersion might bear a certain potential with regard to the evaluation of modified convective gas transport in diseased lungs and clinical diagnosis of several pulmonary insufficiencies. At the same time, it was restrictively stated that the FEV_1/FVC quotient disposes of disease-specific sensitiveness largely comparable to that of aerosol bolus inhalation, but causes much lower medical expenses (21-29).

Besides the experimental investigation of aerosol bolus dispersion and its dependence on lung morphometry also theoretical approaches to this phenomenon were undertaken in the past decades (15-20,30-34). These models were founded either on the simple concept of effective diffusivities introduced by Scherer (30) or on the more complex numerical considerations made by Sarangapani & Wexler (31). Independent of the used mathematical approach, they could generate mostly reliable and experimentally supported predictions, according to which aerosol bolus dispersion may not solely be quantified by the peak half-width, but also by additional statistical parameters (standard deviation, skewness, peak mode-shift, particle deposition) exhibiting a partly higher sensitiveness to any structural changes in the lungs.

Main objectives of the present contribution

The work presented here pursues two main goals: First, the theoretical approach of emphysema originally developed by Sturm & Hofmann (35) is subjected to a brief recapitulation. Second, the potential of aerosol bolus dispersion as diagnostic tool in lungs being affected by different manifestations of emphysema (without COPD) is hypothetically tested and thoroughly discussed. Here, possible preferences of the inhalation technique for future clinical applications should be worked out.

Materials and methods

Brief description of the emphysema model used for theoretical computations

The emphysema approach used in this contribution was implemented in the stochastic morphometric lung model formerly introduced by Koblinger & Hofmann (36,37). Within this theoretical approximation, air-conducting structures are commonly scaled to a functional residual capacity of 3,300 mL, corresponding to the average lung size of a male Caucasian adult (38). The highly specific lung architecture being related to the different manifestations of emphysema was realized by the definition of a minimal and maximal alveolar diameter (d_{min}, d_{max}). In addition, the diameter of a sphere approximating the closing sac at the end of the inhalation path was determined numerically (d_{sac}). For predefined alveolated airways (depending on the manifestation of emphysema), diameters of the alveoli were varied by randomly selecting respective values from a Gaussian distribution, which ranged from d_{min} to d_{max}. Diameters of the closing sacs, on the other hand, were commonly kept constant (35).

Morphometric specificities of single types of emphysema were theoretically approximated in the way illustrated in *Figure 2*. In the lungs of healthy subjects, alveolar diameters were thought to adopt a constant value of 0.250 mm (36-38). Centriacinar emphysema (*Figure 2B*) was simulated by a random variation of alveolar diameters from the first alveolated airway generation m to airway generation $m+k-l$. Within this formal concept, $m+k$ denotes the last generation of the airway path, whereas l represents a random integer number ranging from 3 to k. In the case of paraseptal emphysema (*Figure 2C*), modification of alveolar diameters was confined to the airway generations $m+k$ to $m+k-3$, thereby expressing the highly peripheral occurrence of this manifestation. Additionally, the closing sacs were enlarged within a physiologically meaningful range. With regard to panacinar emphysema (*Figure 2D*), modifications of the alveolar diameters were thought to affect all alveolated airways (airway generations m to $m+k$). Closing sacs were subject to a similar enlargement as constituted for paraseptal emphysema. Simulation of bullous emphysema took place in the same way as that of panacinar emphysema, but d_{max} and d_{sac} were submitted to a further increase (35).

As outlined in the introduction, emphysema commonly results from the destruction of alveolar walls and the increase of the peripheral air volume at the expense of the number of alveoli. Alveolar number is dramatically reduced not only by the disintegration of septa, but also by the collapse of healthy alveoli being situated adjacent to emphysematous structures (*Figure 3*). This phenomenon is accounted for by definition of a degree of alveolarization (p_{alv}). In emphysematous lungs, this parameter is subject to a

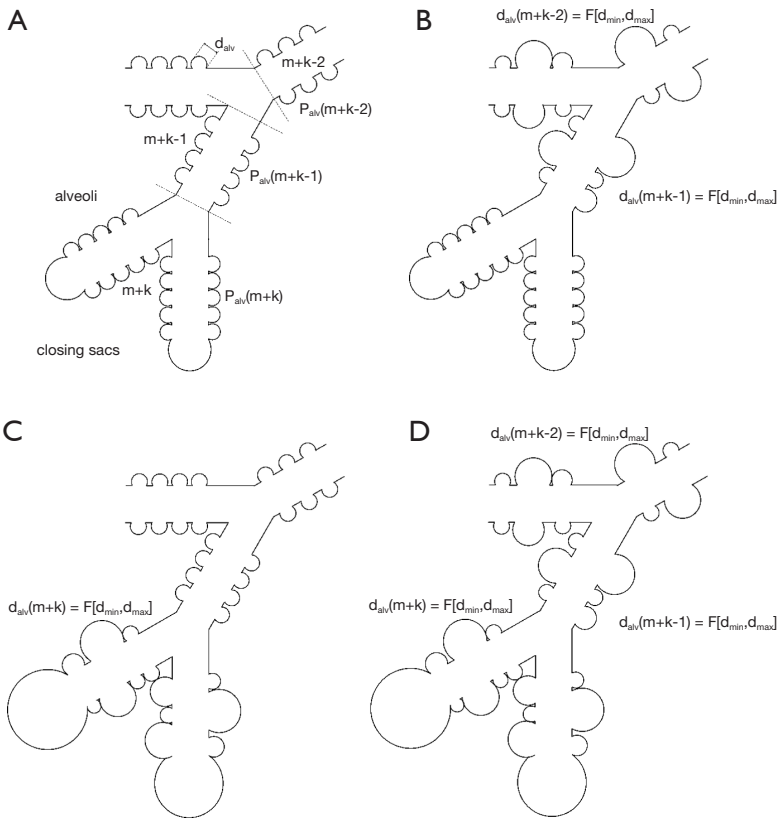

Figure 2 Mathematical and geometric approach to the alveolar structure of healthy subjects (A) and the different types of emphysematous modifications of the peripheral region: (B) centriacinar emphysema, (C) paraseptal emphysema, (D) panacinar and bullous emphysema (35). See text for a more detailed description.

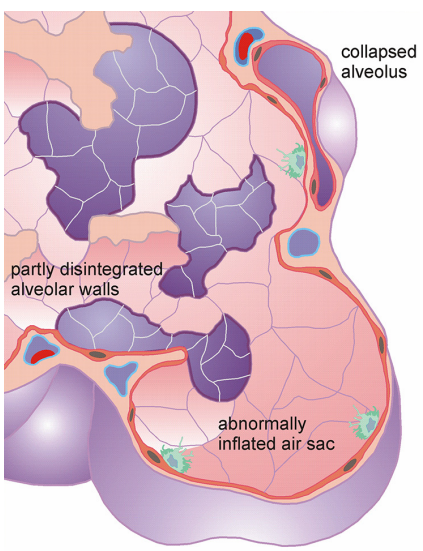

Figure 3 Sketch illustrating the contrast between abnormally inflated alveolar structures on the one side and collapsed air sacs on the other. All these scenarios are considered in the theoretical model by definition of a so-called degree of alveolarization (p_{alv}).

decrease with respect to healthy respiratory structures. The extent of the reduction depends on several morphological factors, among which the quotient between mean alveolar diameter in emphysematous lungs and alveolar diameter in healthy lungs, the quotient between the functional residual capacities in diseased and normal lungs as well as the quotient between the respective diameters of the closing sacs play a superior role. As a special feature of the model, alveolarization may also undergo a slight increase, if collapsed alveoli are reactivated during the successive enhancement of FRC at medium to late stages of emphysema (35).

Mathematical model of aerosol bolus dispersion

Since the stochastic aerosol bolus model has been already subjected to comprehensive descriptions in previous publications (15-20,33,34,39,40), only those features being most essential for an understanding of the entire theoretical concept will be outlined here. It has to be mentioned in

advance, however, that the dispersion of inspired aerosol boluses mainly results from convective gas mixing in the air-conducting structures and alveoli. This phenomenon may be approximated by so-called effective diffusivities, which have to be computed separately for inhalation [$D_{eff}(I)$] and exhalation [$D_{eff}(E)$]. From a mathematical point of view, these two parameters are expressed by the following equations (26):

$$D_{eff}(I) = \chi(D + 1.08ud) \quad [1]$$

and

$$D_{eff}(E) = \chi(D + 0.37ud). \quad [2]$$

In the formulae noted above, χ has to be regarded as specific correction factor for small particles, whereas D, u, and d, respectively, denote the diffusion coefficient (cm^2/s), the mean velocity of the inspired air stream in a specified airway tube (cm/s), and the cylindrical diameter of that bronchial structure (cm). According to the equations effective diffusivities positively correlate with all these factors. The time required by an aerosol bolus for the passage of a given airway tube with the length L may be obtained from the Gaussian probability distribution

$$P(t) = 1/[D_{eff}(2\pi)] \exp[-(L - ut)^2/2(D_{eff}t)^2]. \quad [3]$$

Selection of specific transit times is conducted according to the random number concept, which is applied to the related probability density function of the distribution noted above (15-20).

In the alveolar region, aerosol bolus dispersion is mainly determined by the mixing process between inhaled and residual air. According to the model presented here ideal mixing between these air volumes may be distinguished from complete absence of any mixing phenomena. The latter case is simulated with the help of the so-called "first-in-last-out" concept, according to which particles entering an alveolus at the very beginning of the inhalation phase will leave this respiratory structure again at the very end of the breath cycle (15-20,33,34,39,40). As real alveolar aerodynamics vary between ideal and non-mixing, an empirical mixing factor was defined (37), which was committed to a constant value of 0.25, corresponding to 25% ideal mixing and 75% non-mixing.

Besides the half-width of the exhaled aerosol bolus also the standard deviation, skewness, and mode-shift of the expired particle peak were computed. Respective statistical calculations were commonly based on normalized mathematical moments and were carried out according to well defined standard procedures described in earlier contributions (12,13,15-20). Particle deposition from the aerosol bolus was modelled by using the well-proven transport and deposition model outlined by Koblinger & Hofmann (37) and assuming Brownian motion, sedimentation, and inertial impaction as main deposition mechanisms seizing the particulate substances (41-45).

Model parameters used in this study

Modeling predictions were generated by assuming a constant breath-cycle time of 8 s with symmetric inhalation and exhalation and the absence of an intercalated breath-hold. Tidal volume was assessed with 1000 mL resulting in an inspiration flow rate of 250 mL/s. Half-width of the inhaled aerosol bolus was committed to 50 mL, which corresponds to a time interval of 0.2 s at the specified frame conditions. Insertion of the aerosol peak into the inspired air took place after 100 mL (0.4 s), 200 mL (0.8 s), 300 mL (1.2 s), 400 mL (1.6 s), 500 mL (2.0 s), 600 mL (2.4 s), 700 mL (2.8 s), and 800 mL (3.2 s). Inhaled boluses were injected with monodisperse spherical particles with a diameter of 0.84 μm (12) and unit-density (1 g/cm^3).

Results

Aerosol bolus dispersion in lungs affected by different types of emphysema

For an effective presentation of data predicted by the model, aerosol bolus parameters such as half-width of the exhaled particle peak (mL), standard deviation (mL), skewness, and mode-shift were plotted as functions of the so-called volumetric lung depth (VLD) (*Figures 4,5*). This factor may be regarded as volumetric measure indicating the position of the aerosol bolus within the inhaled air stream. As it represents the volumetric distance from the peak center to the end of inspiration (15-20,33,34), low values for VLD correspond to shallow bolus inhalation, whereas high values mark deep bolus inhalation.

Concerning the theoretically measured half-width of the exhaled aerosol bolus and its dependence on VLD, respective functions calculated for healthy lungs and different manifestations of emphysema are illustrated in *Figure 4A*. In general, patients suffering from emphysema produce higher dispersion of the inspired aerosol pulse than healthy subjects. Related discrepancies of the bolus half-widths become more accentuated with increasing VLD. Among the single types of the disease, bolus dispersion continuously increases from centriacinar and paraseptal emphysema over panacinar emphysema to bullous

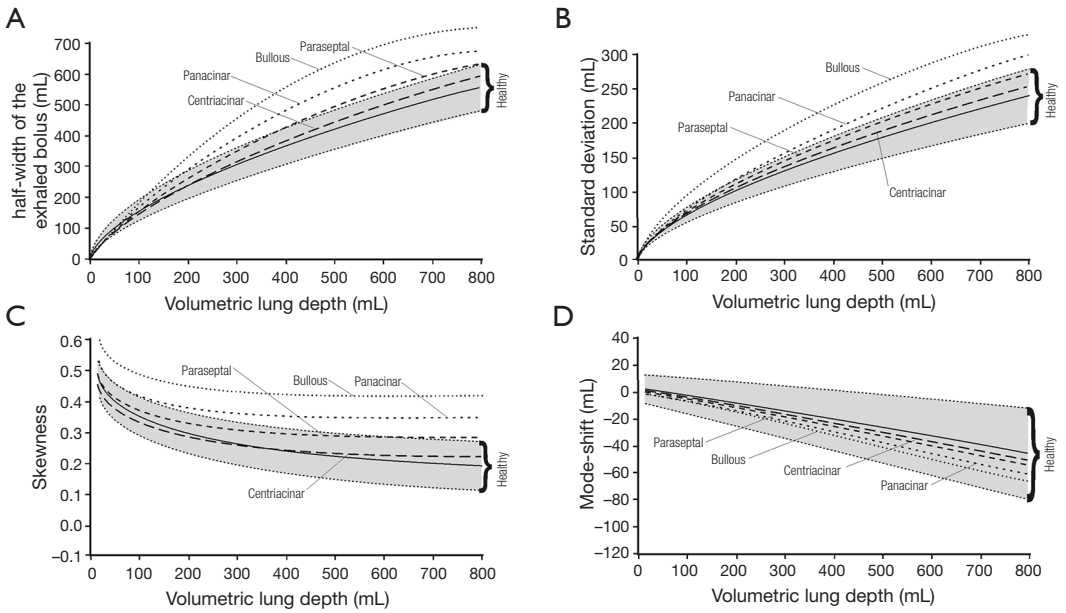

Figure 4 Statistical parameters obtained from the aerosol bolus dispersion model and their expression as functions of the volumetric lung depth (VLD). (A) Half-width of the exhaled bolus; (B) standard deviation; (C) skewness; (D) mode-shift.

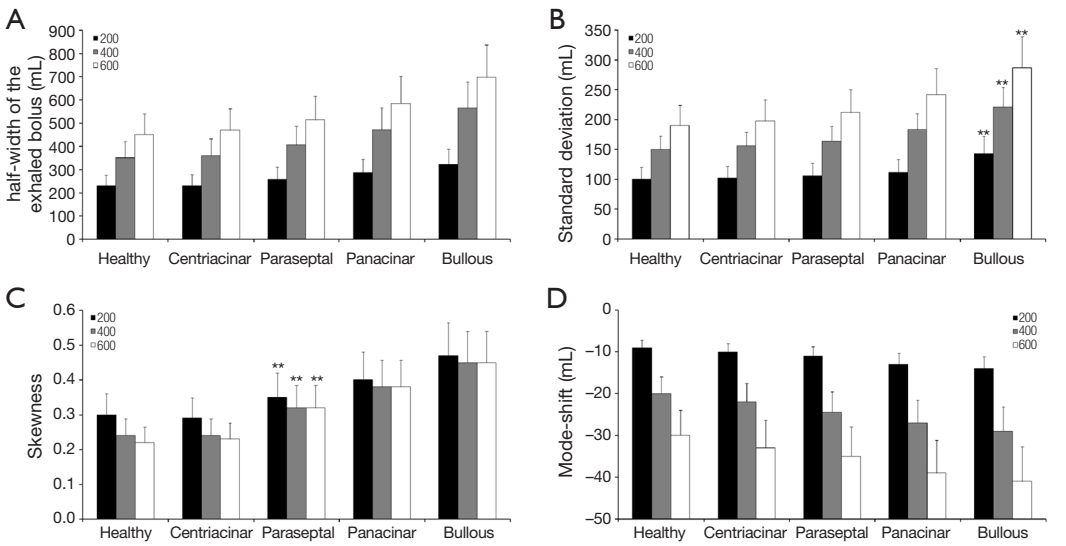

Figure 5 Comparison of statistical parameters (VLD: 200, 400, and 600 mL) of aerosol bolus dispersion predicted for healthy and diseased lungs. (A) Half-width of the exhaled bolus; (B) standard deviation; (C) skewness; (D) mode-shift (**,P< 0.01).

emphysema. At a VLD of 400 mL, respective bolus half-widths of the four manifestations amount to 365±49 mL, 406±56 mL, 472±68 mL, and 565±82 mL. As indicated in *Figure 5A*, at a VLD of 600 mL half-width of bullous emphysema differs significantly (P<0.05) from those computed for the other manifestations of emphysema.

Standard deviation of the exhaled aerosol bolus exhibits a dependence on VLD and manifestation of emphysema, which is very similar to that of the half-width (*Figure 4B*). In concrete terms, this statistical parameter is subject to an increase from 70±8 mL (VLD =100 mL) to 230±25 mL (VLD =800 mL) in healthy probands. In patients suffering from centriacinar or paraseptal emphysema, standard deviation is continuously enhanced from 71±7 mL (73±9 mL)

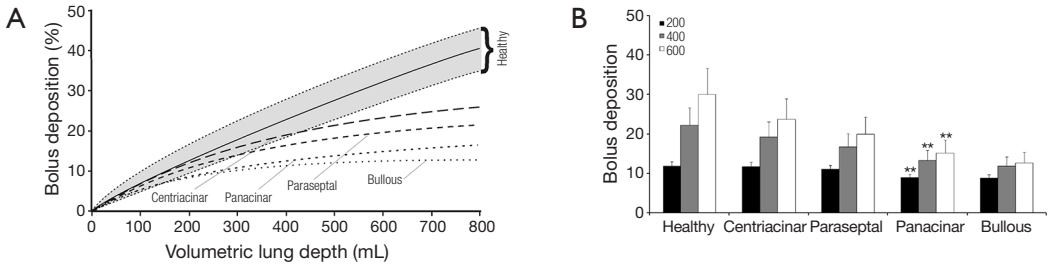

Figure 6 Deposition of particles from aerosol boluses inspired by healthy subjects and emphysema patients. (A) Deposition curves as functions of VLD; (B) comparison of total deposition values predicted four three different VLDS (200, 400, and 600 mL; **, P< 0.01).

to 236±34 mL (253±36 mL). In lungs affected by centriacinar emphysema, the parameter ranges from 77±11 mL to 289±54 mL, whereas bullous emphysema generates values varying between 82±15 mL and 324±67 mL and thus differs with high significance from the other three types (P<0.01) (*Figure 5B*).

With regard to skewness, representing an indicator of increasing peak asymmetry during pulmonary aerosol bolus transport, also some considerable differences between healthy and diseased lungs could be predicted (*Figure 4C*). In concrete terms, this statistical parameter develops from 0.35±0.04 (VLD =100 mL) to 0.2±0.05 (VLD =800 mL) in healthy subjects. In patients with emphysematous lungs, respective values of skewness measured after shallow bolus inhalation commonly range from 0.33±0.04 (centriacinar) to 0.5±0.05 (bullous), whilst values computed after deep bolus inhalation vary between 0.23±0.05 (centriacinar) and 0.43±0.06 (bullous). Here, differences between centriacinar and paraseptal emphysema are already valuable as highly significant (*Figure 5C*).

Mode-shift indicating a certain displacement of the aerosol peak during its transport through the air-conducting structures of the lungs generally develops from +4.0±10.0 (VLD =100 mL) to -40.0±35.0 (VLD =800 mL) in healthy lungs (*Figure 4D*). In emphysematous lungs, values of this parameter determined for shallow bolus inhalation plot within an interval ranging from –2.4±5.4 to +2.3±6.1, whilst values determined for deep bolus inspiration commonly vary between –43.1±32.4 and –61.5±41.2. As depicted in *Figure 5D*, bullous emphysema develops values for the mode-shift not differing significantly from those predicted for centriacinar and paraseptal emphysema.

Particle deposition from the aerosol bolus

Another indicator for the distinction between healthy and diseased lungs is given by the amount of particles undergoing deposition during pulmonary aerosol bolus transport. As illustrated in *Figure 6A*, particle deposition exponentially increases with the VLD and ranges from 5.4±1.2% (VLD =100 mL) to 38.2%±6.7% (VLD =800 mL) in healthy probands. A completely different situation becomes apparent in patients suffering from emphysema, where deposition of inhaled particles is generally subject to a remarkable decline. Starting with centriacinar emphysema, deposition of 0.84 µm particles assumes values between 5.3%±1.4% and 25.2%±6.5%, whereas in lungs affected by paraseptal emphysema deposition of the same particles increases from 5.1%±1.2% to 19.8%±4.7%. Between these two disease manifestations, statistical discrepancies may be evaluated as insignificant, whilst differences from healthy controls are partly remarkable (*Figure 6B*).In patients developing panacinar emphysema, particle deposition ranges from 4.9%±1.1% to 15.2%±4.5% and thus experiences a further highly significant reduction (P<0.01). A similar situation becomes true in the case of bullous emphysema, where deposition varies between 4.6%±0.8% and 13.8%±4.1%, thereby differing insignificantly from that of panacinar emphysema.

Discussion and conclusions

Due to its worldwide impact emphysema has produced immense economic costs for national and international health care infrastructures during the past decades (1-8,35). Modern lung medicine commonly distinguishes four types of emphysema, which develop in different parts of the respiratory compartment and are moreover characterized by variable intensities with regard to the enzymatic disintegration of the alveolar walls and the associated formation of extremely enlarged air sacs distal to the terminal bronchioles (6-10). Currently, an essential demand

of pneumologists on inhalation experiments includes the inexpensive and, even more important, unequivocal diagnosis of the emphysematous manifestation in a patient suffering from this calamitous disease. Although measurement of the FEV_1/FVC quotient has crystallized out as highly effective method for emphysema screening, it still bears some inaccuracies, which can be largely broached by application of an additional or alternative diagnosis technique. Here, aerosol bolus inhalation comes into play, because this method requires rather low technical expenditure and provides a multitude of measurable statistical parameters for diagnostic purposes (12-29).

The present contribution has to be mainly understood as preliminary study for evaluating the possible potential of aerosol bolus inhalation for the secure diagnosis of emphysematous modifications in the distal lungs. As outlined in a few theoretical (15-20) and experimental investigations (21-29), aerosol bolus dispersion, being quantifiable by four independent statistical parameters (half-width of the exhaled bolus, standard deviation, skewness, mode-shift), exhibits a certain sensitiveness with regard to significantly enlarged pathological structures of the lung periphery. In addition, some hypothetical examinations (19,20) already indicated the enhanced importance of particle deposition from the aerosol bolus as advanced characteristic for medical diagnosis. Previous research, however, came to the conclusion that emphysematous lungs commonly produce both enhanced aerosol bolus dispersion and declined particle deposition with respect to healthy respiratory structures (19,20,27-29). Related experiments and theoretical predictions did not carry out any differentiation between single manifestations of emphysema, so that the present study receives a somewhat pioneering character.

As underlined by the hypothetical results presented here, centriacinar and paraseptal emphysema, both locally restricted manifestations of the disease (*Figures 1*,*2*), exhibit changes of the bolus parameters, which all together plot within the variation field of healthy lungs defined by intra- and inter-subject variability of the lung parameters (*Figures 4A*,*5A*). Panacinar and bullous emphysema, on the other hand, produce at least three bolus parameters (half-width, standard deviation, skewness) that plot far outside this area predicted for the normal lung. In general, changes of the statistical parameters with respect to the healthy lung continuously increase from centriacinar over paraseptal to panacinar emphysema and attain their maximum with the bullous manifestation. From a physical point of view, enhancement of aerosol bolus dispersion correlates with the extent of alveolar destruction and peripheral formation of air pouches insofar as inhaled air becomes trapped in these structures for a longer period of time, causing a remarkable contribution of intra-alveolar air mixing processes to the successive spreading and deformation of the particle peak (15-20). Differences between centriacinar and paraseptal emphysema are chiefly founded upon the circumstance that the degree of alveolarization positively correlates with airway generation. This means that respiratory bronchioles directly following the terminal bronchioles are marked by rather low degrees of alveolarization, whereas most distal respiratory bronchioles are completely surrounded by alveoli and thus bear an increased susceptibility for emphysematous changes (19,20,35).

Particle deposition predicted for all four emphysematous manifestations noticeably differs from that of healthy lungs (*Figure 5*) and thus seems to represent a more reliable diagnostic indicator than most statistical parameters being directly associated with aerosol bolus dispersion. As already demonstrated in previous deposition studies (41-58), size of the alveolar structures has a remarkable influence on particle deposition insofar as intra-alveolar distances become much greater and particulate substances require more time to hit the alveolar walls by diffusive or sedimentative transport. Here it has to be clearly noted that particle deposition may only represent an appropriate diagnostic parameter in the case of emphysema developing a valuable predominance over COPD. In the opposite case, reduced particle deposition in the emphysematous structures is largely compensated by increased deposition in the narrowed bronchial and bronchiolar airways (19,20,35).

The theoretical results presented here lead to the conclusion that aerosol bolus inhalation might be partly classified as technique bearing a certain potential for the clinical diagnosis of lung insufficiencies. In the case of the unaccompanied occurrence of emphysema and the absence of COPD, aerosol bolus dispersion generated in diseased lungs can be well distinguished from that produced in healthy lungs. Additionally, different manifestations of emphysema can be faintly diagnosed with the experimental method. A rather trustworthy parameter for a more accurate differentiation between the emphysema types is given by particle deposition, which continuously increases from centriacinar to bullous emphysema. It has to be stated very clearly that theoretical computations certainly reproduce a somewhat idealistic case, which is never attained by related experiments. Here, however, models may be interpreted as tools supporting the improvement of specific inhalation techniques.

Acknowledgments

None.

Footnote

Conflicts of Interest: The author has no conflicts of interest to declare.

References

1. O'Donnell MD, O'Connor CM, FitzGerald MX, et al. Ultrastructure of lung elastin and collagen in mouse models of spontanous emphysema. Matrix Biol 1999;18:357-60.
2. Waddell TK. Treatment of patients with lung cancer and severe emphysema: lessons from lung volume reduction surgery. Surg Oncol 2002;11:201-6.
3. Cardoso WV, Sekhon HS, Hyde DM, et al. Collagen and elastin in human pulmonary emphysema. Am Rev Respir Dis 1993;147:975-81.
4. Fitzpatrick M. Studies on human pulmonary connective tissue. Am Rev Respir Dis 1967;96:254-65.
5. Foronjy R, D'Armiento J. The role of collagenase in emphysema. Respir Res 2001;2:348-52.
6. Laurell CD, Erikson S. The electrophoretic a1-globulin pattern of serum in alpha 1–antitrypsin deficiency. Scand J Clin Lab Invest 1963;15:132-40.
7. Janus ED, Phillips NT, Carrell RW. Smoking, lung function, and alpha1-AT deficiency. Lancet 1985;1:152-4.
8. Eidelman D, Saetta MP, Ghezzo H, et al. Cellularity of the alveolar walls in smokers and its relation to alveolar destruction. Functional implications. Am Rev Respir Dis 1990;141:1547-52.
9. Haas F, Sperber-Haas S. The Chronic Bronchitis and Emphysema Handbook. Hoboken: John Wiley & Sons, 2000.
10. Divisi D, Battaglia C, Di Francescantonio W, et al. Giant bullous emphysema resection by VATS. Analysis of laser and stapler techniques. Eur J Cardiothorac Surg 2002;22:990-4.
11. Luijendijk SC, van der Grinten CP. The ratio of the alveolar ventilations of SF6 and He in patients with lung emphysema and in healthy subjects. Respir Physiol Neurobiol 2002;130:69-77.
12. Heyder J, Blanchard JD, Feldman HA, et al. Convective mixing in human respiratory tract: estimates with aerosol boli. J Appl Physiol 1988;64:1273-8.
13. Brown JS, Gerrity TR, Bennet WD, et al. Dispersion of aerosol boluses in the human lung: dependence on lung volume, bolus volume, and gender. J Appl Physiol 1995;79:1787-95.
14. Schulz H, Heilmann P, Hillebrecht A, et al. Convective and diffusive gas transport in canine intrapulmonary airways. J Appl Physiol 1992;72:1557-62.
15. Rosenthal FS, Blanchard JD, Anderson PJ. Aerosol bolus dispersion and convective mixing in human and dog lungs and physical models. J Appl Physiol 1992;73:862-73.
16. Sturm R, Pawlak E, Hofmann W. Monte-Carlo-Modell der Aerosolbolusdispersion in der menschlichen Lunge – Teil 1: Theoretische Modellbeschreibung und Anwendung. Z med Phys 2007;17:127-35.
17. Sturm R, Pawlak E, Hofmann W. Monte-Carlo-Modell der Aerosolbolusdispersion in der menschlichen Lunge – Teil 2: Modellvorhersagen für die kranke Lunge. Z med Phys 2007;17:136-43.
18. Hofmann W, Pawlak E, Sturm R. Semi-empirical stochastic model of aerosol bolus dispersion in the human lung. Inhal Toxicol 2008;20:1059-73.
19. Sturm R. Aerosol bolus dispersion in healthy and asthmatic children—theoretical and experimental results. Ann Transl Med 2014;2:47.
20. Sturm R. Aerosol bolus inhalation in subjects with different age – a theoretical approach. Comp Math Biol 2014;3:7.
21. Anderson PJ, Hardy KG, Gann LP, et al. Detection of small airway dysfunction in asymptomatic smokers using aerosol bolus behavior. Am J Resp Crit Care Med 1994;150:995-1001.
22. Anderson PJ, Blanchard JD, Brain JD, et al. Effect of cystic fibrosis on inhaled aerosol boluses. Am Rev Resp Dis 1989;140:1317-24.
23. Blanchard JD. Aerosol bolus dispersion and aerosol-derived airway morphometry: assessment of lung pathology and response to therapy, part 2. J Aerosol Med 1996;9:183-205.
24. Schulz H, Eder G, Heyder J. Lung volume is a determinant of aerosol bolus dispersion. J Aerosol Med 2003;16:255-62.
25. McCawley M, Lippmann. Development of an aerosol dispersion test to detect early changes in lung function. Am Ind Hyg Assoc J 1988;49:357-66.
26. Schulz H, Schulz A, Brand P, et al. Aerosol bolus dispersion and effective airway diameters in mildly asthmatic children. Eur Respir J 1995;8:566-73.
27. Verbanck S, Schuermans D, Vincken W, et al. Saline aerosol bolus dispersion. I. The effect of acinar airway alteration. J Appl Physiol 2001;90:1754-62.

28. Kohlhäufl M, Brand P, Rock C, et al. Noninvasive Diagnosis of Emphysema. Am J Resp Crit Care Med 1999;160:913-8.
29. Kohlhäufl M, Brand P, Scheuch G, et al. Aerosol Morphometry and Aerosol Bolus Dispersion in Patients with CT-Determined Combined Pulmonary Emphysema and Lung Fibrosis. J Aerosol Med 2000;13:117-24.
30. Scherer PW, Shendalman LH, Greene NM, et al. Measurement of axial diffusivities in a model of the bronchial airways. J Appl Physiol 1975;38:719-23.
31. Sarangapani R, Wexler AS. Modeling aerosol bolus dispersion in human airways. J Aerosol Sci 1999;30:1345-62.
32. Lee JW, Lee DY, Kim WS. Dispersion of an aerosol bolus in a double bifurcation. J Aerosol Sci 2000;31:491-505.
33. Darquenne C, Brand P, Heyder J, et al. Aerosol dispersion in human lung: comparison between numerical simulations and experiments for bolus tests. J Appl Physiol 1997;83: 966-74.
34. Sturm R. Aerosol bolus inhalation as technique for the diagnosis of various lung diseases – a theoretical approach. Comp Math Biol 2014;3:2.
35. Sturm R, Hofmann W. Stochastic simulation of alveolar particle deposition in lungs affected by different types of emphysema. J Aerosol Med 2004;17:357-72.
36. Koblinger L, Hofmann W. Analysis of human lung morphometric data for stochastic aerosol deposition calculations. Phys Med Biol 1985;30:541-56.
37. Koblinger L, Hofmann W. Monte Carlo modeling of aerosol deposition in human lungs. Part I: Simulation of particle transport in a stochastic lung structure. J Aerosol Sci 1990;21:661-74.
38. International Commission on Radiological Protection (ICRP). Human Respiratory Tract Model for Radiological Protection, Publication 66. Oxford: Pergamon Press, 1994.
39. Schulz H, Schulz A, Brand P, et al. Aerosol bolus dispersion and effective airway diameters in mildly asthmatic children. Eur Respir J 1995;8:566-73.
40. Keefe MJ, Bennett WD, DeWitt P, et al. The effect of ozone exposure on the dispersion of inhaled aerosol boluses in healthy human subjects. Am Rev Respir Dis 1991;144:23-30.
41. Sturm R. Bioaerosols in the lungs of subjects with different ages - part 1: deposition modeling. Ann Transl Med 2016;4:211.
42. Sturm R. A computer model for the simulation of fiber-cell interaction in the alveolar region of the respiratory tract. Comput Biol Med 2011;41:565-73.
43. Sturm R. Theoretical models of carcinogenic particle deposition and clearance in children's lungs. J Thorac Dis 2012;4:368-76.
44. Sturm R. Deposition and cellular interaction of cancer-inducing particles in the human respiratory tract: Theoretical approaches and experimental data. Thoracic Cancer 2010;4:141-52.
45. Sturm R, Hofmann W. A theoretical approach to the deposition and clearance of fibers with variable size in the human respiratory tract. J Hazard Mater 2009;170:210-8.
46. Sturm R. Theoretical approach to the hit probability of lung-cancer-sensitive epithelial cells by mineral fibers with various aspect ratios. Thoracic Cancer 2010;3:116-25.
47. Sturm R. Theoretical and experimental approaches to the deposition and clearance of ultrafine carcinogens in the human respiratory tract. Thoracic Cancer 2011;2:61-8.
48. Sturm R. Theoretical models for the simulation of particle deposition and tracheobronchial clearance in lungs of patients with chronic bronchitis. Ann Transl Med 2013;1:3.
49. Sturm R. Modeling the deposition of bioaerosols with variable size and shape in the human respiratory tract - A review. J Adv Res 2012;3:295-304.
50. Sturm R, Hofmann W. A computer program for the simulation of fiber deposition in the human respiratory tract. Comput Biol Med 2006;36:1252-67.
51. Sturm R. Theoretical models for dynamic shape factors and lung deposition of small particle aggregates originating from combustion processes. Z med Phys 2010;20:226-34.
52. Sturm R. Nanotubes in the respiratory tract - Deposition modeling. Z med Phys 2015;25:135-45.
53. Sturm R. A stochastic model of carbon nanotube deposition in the airways and alveoli of the human respiratory tract. Inhal Toxicol 2016;28:49-60.
54. Sturm R. Inhaled nanoparticles. Phys Today 2016;69:70-1.
55. Sturm R. A computer model for the simulation of nanoparticle deposition in the alveolar structures of the human lungs. Ann Transl Med 2015;3:281.
56. Sturm R. Spatial visualization of theoretical nanoparticle deposition in the human respiratory tract. Ann Transl Med 2015;3:326.
57. Sturm R. Theoretical deposition of nanotubes in the respiratory tract of children and adults. Ann Transl Med 2014;2:6.
58. Sturm R. Theoretical deposition of carcinogenic particle aggregates in the upper respiratory tract. Ann Transl Med 2013;1:25.

Cite this article as: Sturm R. Theoretical diagnosis of emphysema by aerosol bolus inhalation. Ann Transl Med 2017;5(7):154. doi: 10.21037/atm.2017.03.28

